Correlated Dopant Distributions in Delta-Doped Layers

P.M. Koenraad

COBRA Interuniversity Research Institute,
Eindhoven University of Technology
P.O.Box 513, 5600 MB Eindhoven, The Netherlands

Received February 2, 1997

In this paper we discuss the observation of correlations in the spatial distribution of Be atoms in delta doped layers. In Si delta doped samples we show that correlations in the charge distribution occur when DX centers are populated. The mobility enhancement we measure in our structures agrees with the calculated enhancement due to correlations effects.

I. Introduction

In most bulk-grown semiconductors ionized impurities dominate the scattering at low temperature. Modulation doping has been used successfully to suppress the scattering of free electrons on these ionized donor impurities. In this doping technique the ionized donor impurities are spatially separated from the free electron gas resulting in record mobilities of up to $2 \cdot 10^7$ cm^2/Vs. However in low-dimensional structures, like the well-known GaAs/AlGaAs heterostructures, ionized impurities still dominate the scattering of the electrons. However, in these heterostructures the maximum electron density is about $8 \cdot 10^{15}$ cm^{-2}. In many occasions one would like to have a much higher electron densi-ty. Delta doped layers are capable of delivering very high electron densities and have been studied in great detail. The delta doped layer has a thickness of typically 2 nm when the sample is grown at low growth temperature. Due to the high doping concentration the effective Bohr-radii of the doping atoms in the doping layer overlap and no freeze-out of the electrons occurs at low temperature. The thin layer of ionized impurity atoms forms a V-shaped Coulomb potential which has a thickness smaller than the de Broglie wave-length of the electrons and thus 2-D confined levels are formed, see Fig. 1. Normally a few levels are populated with electrons due to the high doping concentration. The strong overlap of the electron wavefunctions with the ionized impurities at the center of the well is reflected in the very low mobility of the electrons. In the lowest confined state we find electron mobility values of typically 1.000 cm^{-2}/Vs. In higher subbands the electron mobility can be quite different due to: 1) a smaller overlap between the electron wavefunction and the ionized impurity distribution 2) a lower Fermi-velocity of the electron, 3) a different screening.

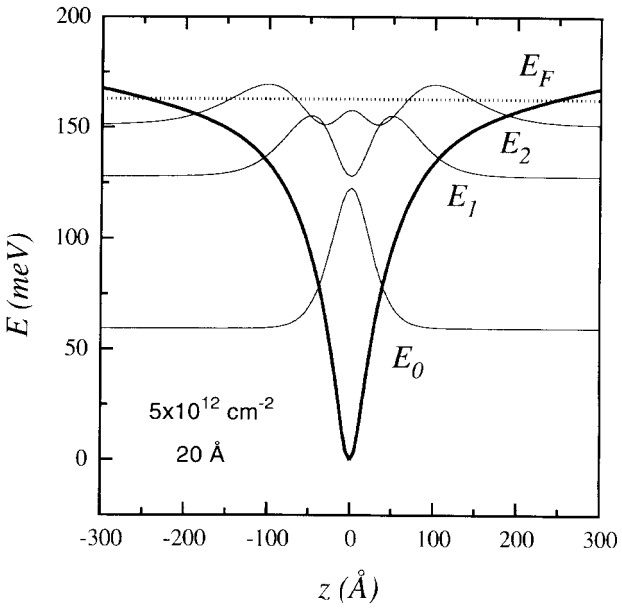

Figure 1. Potential diagram showing the conduction band (thick line), probability distributions of the electrons in the confined states (thin lines) and Fermi Energy (dashed line) in a delta doped structure. The doping layer is 2 nm thick and has a doping concentration of $5 \cdot 10^{12}$ cm^{-2}.

A few decennia ago it has been proposed that the mobility in bulk doped samples might be enhanced due to ordering in the spatial distribution of the ionized impurities [1]. It is a well-known fact that ordered, or correlated, distributions of scatterers lead to a strong

reduction of the scattering. For instance electrons in a semiconductor crystal are not scattered by the crystal itself but only by the imperfections in the crystal like: (neutral) impurities, growth defects, alloy fluctuations and phonons. In this paper we will discuss results we have obtained in delta doped layers where, due to the very high doping concentration, the ionized impurities interact with each other and thus give rise to correlations in the distribution of ionized impurities. These correlations result in an enhanced mobility.

II. Correlations in the spatial distribution of Be-atoms studied by X-STM

With present day growth techniques like MBE, CBE etc. atomically sharp interfaces and doping profiles can be grown. The quality of the interfaces and their composition can be assessed at the atomic scale by cross-sectional Scanning Tunneling Microscopy (X-STM)[2]. In a X-STM setup the samples are cleaved under UHV conditions ($P < 10^{-11}$ torr) -along either the (110) or the (1-10) plane. Because the two latter planes are parallel to the [001] growth direction we can image a cross-section of the grown layer structure. Several authors have recently reported that they were able to observe individual dopant atoms in semiconductor materials by X-STM [3,4]. Therefore one can study both the thickness of a doping layer and the distribution of the dopant atoms within the dopant plane using X-STM.

The Be delta doped sample we have studied with X-STM was grown at 480 ^{o}C on a (001) p+ substrate with an alignment within 0.2^o of the [001] direction. The growth rate was about 1 μm/h (1 monolayer/s). The doping layers where obtained by opening the shutter of the Be furnace during a growth interrupt lasting from 10 up to 360 s. During the growth interrupts the growth surface was kept under an As-flux. In this way a stack of four doping layers was produced with doping concentrations of $3 \cdot 10^{12}$, $10 \cdot 10^{12}$, $30 \cdot 10^{12}$, and $100 \cdot 10^{12}$ cm^{-2} respectively. The highest doping concentration is equal to about 1/6 of a full monolayer. The doping layers were separated by 25 nm of undoped GaAs. The stack of four delta doping layers was repeated 3 times in the structure and the stacks were separated from each other by one or more 2.5 nm thick $Al_{0.2}Ga_{0.8}As$ layers which we used as marker layers. The intended doping concentrations was checked by SIMS measurements and the electrical activity of the dopant atoms was determined by etching CV profiling.

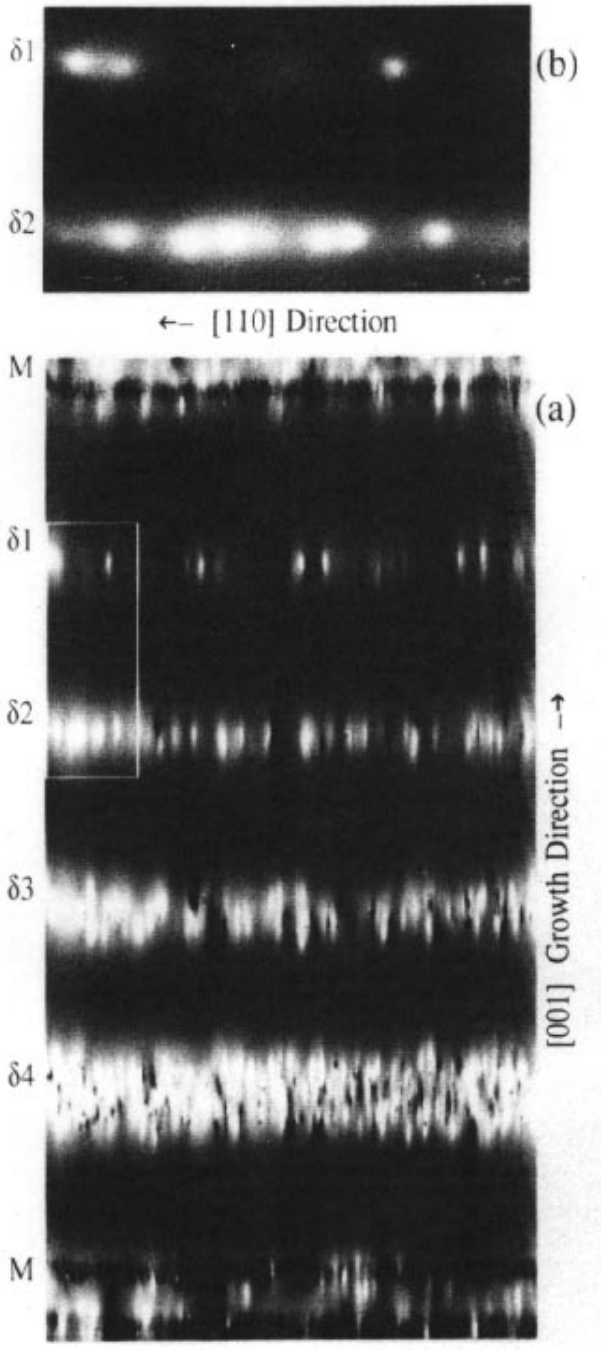

Figure 2. Filled state X-STM image (sample bias -1.0 V) of a structure containing several Be delta doped layers: a) Large scale image (120 nm * 300 nm). The vertical scale (300 nm) is strongly compressed. The active Be atoms appear as white hillocks. b) Enlarged view (31 nm * 54 nm) of the section containing the two doping layers with the lowest doping concentration. Atomic corrugation is observed in both directions allowing an exact position determination of the Be doping atoms.

In Fig. 2 we show a large scale As-related image across a full stack of four delta doping layers. Clearly visible are the white hillocks which are due to individual Be doping atoms and the dark $Al_{0.2}Ga_{0.8}As$ marker

layers. Note that the hillocks are absent between the delta doping layers. Each hillock extends over a few lattice sites because one does not observe the ionized Be atom itself but its Coulomb effect on the electrons tunneling in the immediate surrounding of the Be atom. The radius (2.5 nm) of each hillock is almost equal to the Bohr-radius of an ionized Be atom. The ionized Be atoms closest to the cleaved surface appear most strongest whereas the ones deeper below surface appear weaker. Roughly we are able to observe Be atoms up to a depth of about 1.5 nm below the cleaved surface. The original topographic images allow to determine the position of the Be atoms with atomic resolution. Thus histograms of the position of the dopants can be obtained as shown in Fig. 3.

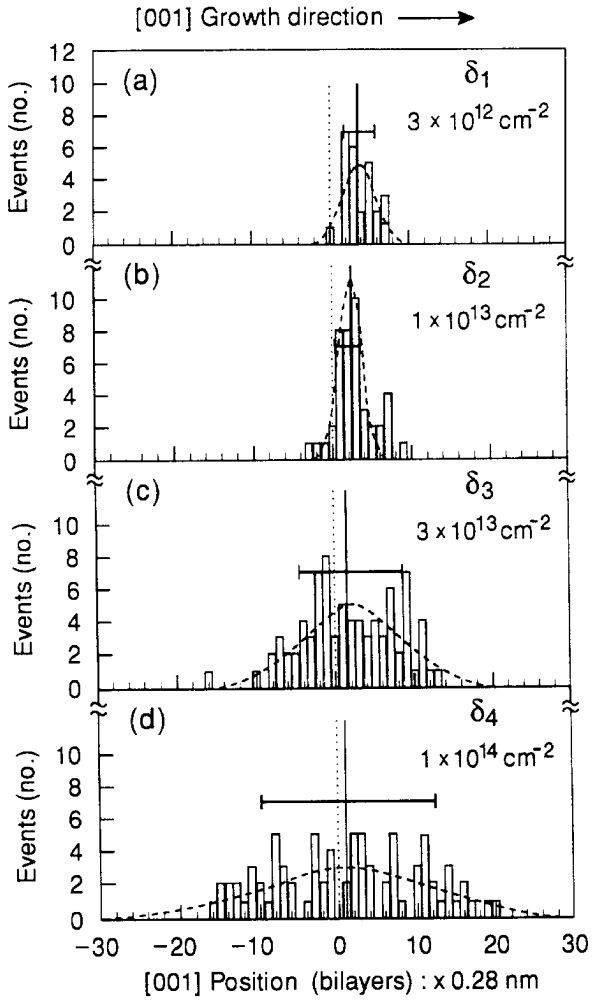

Figure 3. Histogram showing the positions of the Be atoms along the [001] growth direction as observed in the delta layers. The horizontal axis is in bilayers (1 monolayer = 0.28 nm). A Gaussian fit (dotted line) is used to determine the distribution average position (solid vertical line) and width. The intended doping position is indicated by the dotted vertical line.

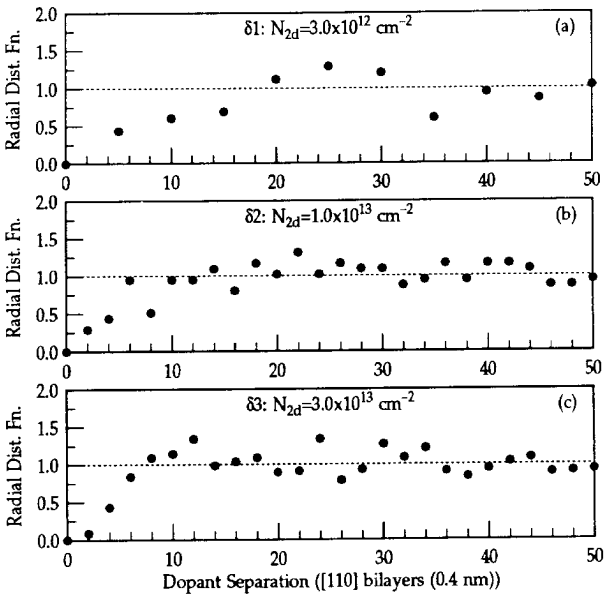

Figure 4. Radial distribution function for the three lowest-concentration doping layers as determined from our X-STM measurements. The dashed line represents the distribution function for a purely random separation.

The histograms demonstrate that the two lowest-concentration delta layers have a near atomic layer thickness of 1 nm. However in the layers with a higher doping concentration a considerable broadening of the layers has occurred. Note that all doping peaks are shifted by about 2 monolayers towards the growth surface. This is probably due to surface segregation. We think that the broadening of the doping layer observed in the layers with highest doping concentrations is due to a mutual Coulomb repulsion between the ionized doping atoms. If this argument holds one would expect an in-plane ordering of the dopant atoms as well. In Fig. 4 we show the radial distribution function (frequency plot of dopant separation of all pairs of dopants) for the three lowest-concentration delta layers. In the case of a purely random distribution we would expect the radial distribution to be equal to 1 for all dopant separations. The distribution functions of the delta layers show clearly that the occurrence of close-spaced neighbors is less probable. In these doping layers with a correlated dopant distribution the mobility of the free holes must be enhanced. It is however rather difficult to prove this enhancement because one cannot easily prepare structures with either an uncorrelated or correlated doping layer. Furthermore accurate results conceming the mobility of the free holes can only be obtained if one can determine the hole mobility in the individual subbands. The subband mobility is obtained

from the amplitude dependence of Shubnikov-de Haas oscillations. However, for p-type delta layers it is impossible to observe these SdH-oscillations because the mobility is extremely low, typically about 100 cm^2/Vs.

III. Effects of spatial correlations in the distribution of charged impurities on the electron mobility

We have shown that in n-type delta doped layers one can successfully obtain both the transport and the quantum mobility in the individual subbands [5]. The results showed that the mobility increases with the subband index. At first sight one would explain this by the stronger overlap of the electron wavefunction in lower subbands with the ionized Si dopant atoms compared to the wavefunctions in the higher subbands. This is however a crude simplification. We have shown that not only the overlap of the electron wavefunction with the ionized donors is important but also the Fermi velocity and, most important, a correct description of the screening [6].

In the case that DX centers saturate the electron density, correlation effects in charge distribution are expected to be present [7,8]. Delta doped structures are ideal to study these correlation effects because there is strong interaction of the electrons with ionized impurities and there is also strong interaction between the ionized impurities themselves. In order that DX centers, and thus correlations in the charge distribution, have an influence on the electron mobility, the Fermi level has to be resonant with the DX level. It is a well established that DX centers in $Al_xGa_{1-x}As$ are resonant with the Γ band at an Al fraction of approximately 0.25 or at a hydrostatic pressure of 20 kbar in GaAs [9]. In order to tune the position of the DX level relative to the Fermi level we have designed [10] and grown [11] delta doped $GaAs/Al_xGa_{1-x}As/GaAs$ barrier structures. In these structures we need only modest hydrostatic pressures to populate the DX center effectively. An example of a delta doped barrier structure is shown in Fig. 5.

There is still concern whether the DX centers traps only one electron (DX^0 model) or two electrons (DX^- model). In either case a mixed valence system exists when a part of the free electrons is trapped by DX states, i.e. part of the Si atoms will have a positive charge (the normal shallow d^+ state) whereas the other part will have a neutral or negative charge (the deep DX^o or DX^- state). The spatial correlations in the charge distribution in a mixed valence system have a twofold effect [10,11]: 1) the position of DX centers is lowered, and 2) the electron mobility increases. Lowering of the DX state means that a lower hydrostatic pressure, Al mole fraction or doping concentration is needed to populate this DX state. Spatial correlations in the charge distribution can be observed in the radial distribution function which was already discussed in the previous paragraph. In the case of the DX^o model there is only one radial distribution function which gives the probability of finding a pair of two positively charged donors at a given separation. The distribution of the neutral donors is not important because the electrons are not scattered by them. In the case of the DX-model there will be three different radial distribution functions showing the probability of finding a pair of two negative, two positive or one positive and one negative Si doping atoms respectively. These radial distribution functions are accounted for in the mobility calculations by the structure factor scaling the scattering rate [10,11]. Because the spatial correlations have a short range character small scattering wave vectors are affected predominantly. Thus we expect that already small correlation effects have a strong influence on the mobility because ionized impurity scattering is most stron-gest for these small scattering wavevectors. As an example we show in Fig. 6 the radial distribution function for the d^+/D^o model as obtained from Monte Carlo simulations. Note that for a smaller free electron concentration (more electrons captured by DX centers) the correlations extend over a larger separation.

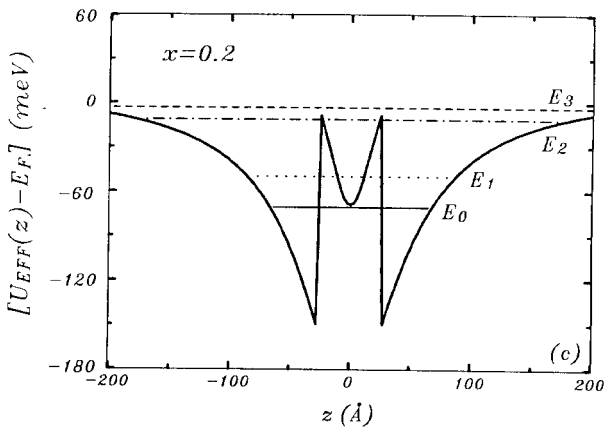

Figure 5. Potential diagram of a delta doped GaAs barrier structure. The energetic position of each confined state is plotted relative to the Fermi energy.

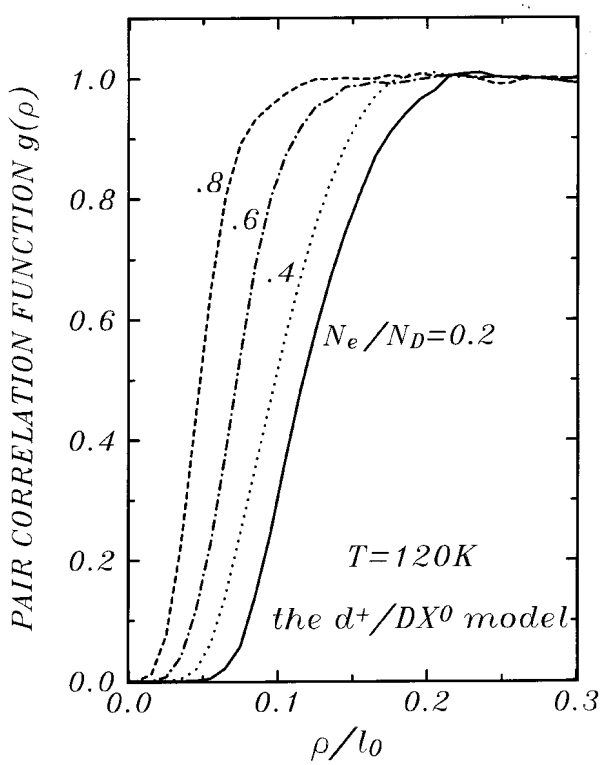

Figure 6. The radial distribution function for the d^+/DX° model as obtained from Monte Carlo simulations. This figure shows the probability of finding a pair of two positively charged donors at a given separation for various fractions of the ratio free electrons to doping Si atoms. The missing electrons are captured by the DX centers.

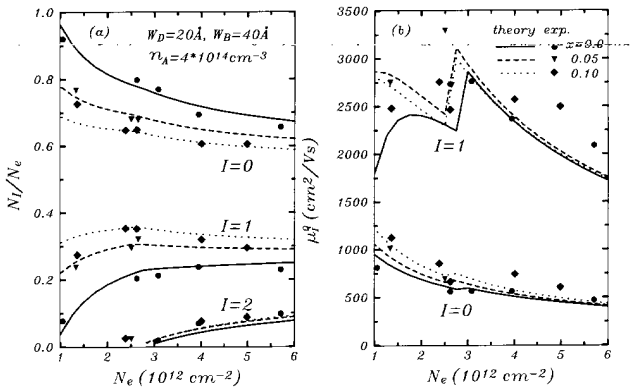

Figure 7. Subband population (a) and quantum mobility (b) in the individual subbands of delta doped $GaAs/Al_xGa_{1-x}As/GaAs$ barrier structures. The experimental results are shown by the symbols, and the theoretical results by lines.

In Fig. 7 we show the population and the quantum mobility in the individual sub-bands of delta doped barrier structures at ambient pressure, having doping concentrations up to $6 \cdot 10^{12}$ cm^{-2} and 4 nm thick $Al_xGa_{1-x}As$ barriers with Al fractions up to 0.1. The population and mobility within each subband was obtained from magneto-transport measurements in fields up to 20 T. The agreement between theory and experiments for both the subband population and the subband mobility is very good. In these structures no DX centers are populated at ambient pressure. Note that the effect of the $Al_xGa_{1-x}As$ barrier is on the mobility is rather small.

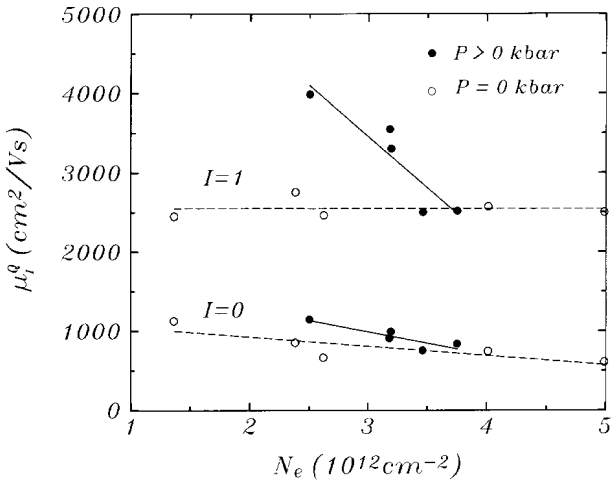

Figure 8. Quantum mobility in the lowest populated subbands as a function of the free electron density for structures with either different doping concentrations (open symbols) or the structure doped at $4.4 \cdot 10^{12}$ cm^{-2} under hydrostatic pressure (solid symbols). The lines are to guide the eye.

Applying hydrostatic pressure to the delta doped $GaAs/Al_{0.1}Ga_{0.9}As/GaAs$ barrier structure having a doping concentration of $4.4 \cdot 10^{12}$ cm^{-2} we are able to vary the total electron density and thus the population of the DX state. Our measurements show a reduction of the free electron density of approximately 30 percent at the maximum hydrostatic pressure of 10 kbar. In the case of that DX centers are negatively charged we find that the position of the DX level is at 320 meV above the Γ conduction band. The observation of a mobility enhancement after the application of hydrostatic pressure does not prove that any spatial correlation in the charge distribution are present. We know from the normal delta doped structures and from the barrier doped structures as well, see Fig. 6, that the mobility also increases when the doping concentration is lowered. If the DX° model applies then the number of scatterers is equal to the number of free electrons (the DX center becomes neutral after capturing an electron) whereas if the DX^- model applies the number of scatterers remains equal to the total doping concentration (the DX center becomes negatively charged after the capture of two electrons). However when we compare the mobility

in sample under pressure with samples at ambient pressure, see Fig. 8, we clearly observe that for the structures with the same electron density, either at ambient pressure or under hydrostatic pressure, that the mobility is enhanced when DX-states are populated. This enhancement must be due to spatial correlations in the charge distribution of the mixed valence system.

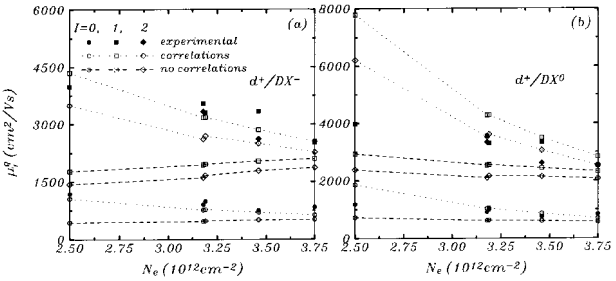

Figure 9. Quantum mobility as a function of the total free electron concentration in the structure doped at $4.4 \cdot 10^{12}$ cm^{-2} and having a 4 nm thick $Al_{0.1}Ga_{0.9}As$ barrier. The experimental results (solid symbols) are compared with theory (open symbols). The theoretical results are shown without (guided by the dashed curves) and with (guided by the dotted curves) inclusion of the correlation effects for the d^+/DX^- (a) and d^+/DX^o (b) models.

Finally in Fig. 9 we show the quantum mobility measured in the structure under hydrostatic pressure as a function of the total free electron density together with the calculated subband mobilities with and without the inclusion of spatial correlation effects. We show calculations for both the d^+/DX^- (a) and d^+/DX^o (b) models. The comparison between experiments and theory show that: correlations exist and can be correctly accounted for in the mobility calculations and 2) the DX center is negatively charged. Note also that the mobility enhancement is about a factor of two in the i=1 subband and a factor of 1.5 in the i=0 subband. From the Monte carlo simulations we noted that the correlations are present up to distances of about 2 nm. In the STM results on the Be delta doped structures we observed correlations up to at least 4 nm. This means that a mobility enhancement in these structures is very plausible.

IV. Conclusions

X-STM measurements on Be-delta doped GaAs samples have shown that spatial correlations in the position of the doping atoms occur up to distances of 4 nm. In Si delta doped $GaAs/Al_xGa_{1-x}/GaAs$ barrier samples we find a clear mobility enhancement when correlations in spatial charge distribution occur.

References

1. I.Y. Yanchev, B.G. Arnaudov and S.K. Evtimova, J. Phys. C **12**, L765 (1979).
2. P.M. Koenraad, M.B. Johnson and H.W.M. Salemink, Materials Sci. For. **196-201**, 1471 (1996).
3. M.B. Johnson, P.M. Koenraad, W.C. van der Vleuten, H.W.M. Salemink and J.H. Wolter, Phys. Rev. Lett. **75**, 1606 (1995).
4. M.C.M.M. van der Wielen, A.J.A. van Roij and H. van Kempen, Phys. Rev. Lett. **76**, 1075 (1996).
5. P.M. Koenraad, chapter 17 in the book *Delta-doping of Semiconductors*, ed by E.F. Schubert, Cambridge University Press, UK (1996).
6. G.Q. Hai, N. Studart, F.M. Peeters, P.M. Koenraad and J.H. Wolter, J. App. Phys. **80**, 5809 (1996).
7. E. Buks, M. Heiblum and H. Shtrikman, Phys. Rev. B **49**, 14790 (1994).
8. Z. Wilamowski, J. Kossut, T. Suski, P. Wisniewski and L. Dmowski, Semicond. Sci. Technol. **6**, B34 (1991).
9. P.M. Mooney, J. Appl. Phys. **67**, R1 (1990).
10. J.M. Shi, P.M. Koenraad, A.F.W. van de Stadt, F.M. Peeters, J.T. Devreese and J.H. Wolter, Phys. Rev. B **54**, 7996 (1996).
11. P. Sobkowicz, Z. Wilamowski and J. Kossut, Semicond. Sci. Technol. **7**, 1155 (1992).